International Journal of Heat and Technology
Vol. 44, No. 2, April, 2026, pp. 803-813
Journal homepage: http://iieta.org/journals/ijht

Predictive Exergy-Based Framework for Assessing Diesel Engine Performance Under Variable Load Conditions Using Diesel-RK

Eihab A. Raouf*, Hussain Sadig

Department of Mechanical Engineering, College of Engineering, Qassim University, Buraydah 51452, Saudi Arabia

Corresponding Author Email: eomer@qu.edu.sa

https://doi.org/10.18280/ijht.440230

Received: 25 January 2026
Revised: 5 April 2026
Accepted: 17 April 2026
Available online: 30 April 2026

Keywords:
diesel engine, Diesel-RK simulation, exergy analysis, exergy destruction, exergy efficiency, variable load

ABSTRACT

The study examines the thermal and exergy behavior of a turbocharged diesel engine over a range of speed–load conditions using Diesel-RK simulation. A post-processing framework was developed to quantify exergy efficiency, destruction, and distribution pathways from Diesel-RK outputs, addressing the lack of built-in exergy analysis in conventional one-dimensional engine simulations. At low-to-moderate speeds, the collected results show that exergy efficiency increases with the increase of load and reaches its maximum value of 35.1% at 2000 rpm under full load, reflecting improved combustion effectiveness and reduced relative heat losses. At high speed (4000 rpm), exergy efficiency decreases significantly to 20.6% due to intensified irreversibilities associated with rapid combustion, increased friction, and constrained heat transfer time scales. Exergy destruction increases strongly with the increase of both speed and load, rising from 19 kW to 364 kW at high-speed full-load operation, reflecting intensified entropy generation driven by rapid heat release and elevated in-cylinder temperature gradients. Operation at moderate speeds under high load produced higher thermodynamic efficiency, reflected in an increased conversion of fuel exergy into brake work. As engine speed increased, the balance shifted toward loss-dominated operation, driven by shorter combustion duration and stronger dissipative effects. The proposed framework supports second-law-based evaluation and provides a basis for performance-oriented optimization of diesel engine operation.

1. INTRODUCTION

The performance of diesel engines has conventionally depended on the first law of thermodynamics to evaluate energy conversion efficiency and fuel consumption [1]. Standard engine analysis frameworks based on energy balance have provided valuable understandings of combustion characteristics, heat transfer, and brake thermal efficiency [2]. First-law-based treatments all treat forms of energy as corresponding and fail to account for the degradation of energy quality associated with irreversible processes during real engine operation [3].

To overcome these limits, exergy analysis based on the second law of thermodynamics has been progressively applied to internal combustion engines (ICE) [4-6]. Exergy analysis provides a quantitative measure of system inefficiencies by identifying their location and magnitude within thermodynamic processes [7]. When applied to diesel engines, it shows that an important portion of the fuel chemical exergy is destroyed due to irreversible combustion, heat transfer across limited temperature differences, and mechanical losses [8].

In ICEs, fuel exergy mainly corresponds to the chemical exergy of the fuel, which represents the maximum theoretical useful work obtainable during ideal combustion with the surrounding environment [9]. Since this maximum work potential exceeds the lower heating value of the fuel, a chemical exergy factor is introduced to relate the chemical exergy of the fuel to its heating value and to accurately quantify the true exergy input in the exergy balance [10]. The fuel is considered the sole source of exergy in ICEs [11]. Intake air functions only as a combustion medium. Heat losses reflect exergy rejected to the surroundings rather than a source term, while the exhaust stream carries the remaining exergy of the fuel [12].

Exergy distribution describes how the fuel exergy is divided between brake work, exhaust flow, heat transfer, and internal losses such as friction [13]. In most cases, only a small portion is recovered as useful work, while the larger share leaves the system through exhaust and heat-transfer pathways [14].

Although exergy analysis has been increasingly applied to ICEs, limited attention has been given to the comprehensive evaluation of exergy distribution and dominant loss mechanisms in diesel engines under varying load conditions using numerical simulation tools. The study evaluates the thermal and exergy behavior of a diesel engine under variable load conditions, with emphasis on exergy distribution and the dominant loss pathways, using Diesel-RK simulation.

2. THEORETICAL BACKGROUND

However, achieving complete conversion of energy into work is thermodynamically impossible due to inherent irreversibilities, which lead to the degradation of energy quality during the conversion process [15]. The portion of energy that represents the maximum useful work obtainable from a system is defined as exergy [16]. Exergy is defined as the maximum useful work a system can deliver as it moves toward equilibrium with its surroundings under reversible conditions [17].

Exergy analysis quantifies where thermodynamic losses occur in energy systems [18]. In ICEs, the losses linked to combustion, heat transfer, and friction enable direct localization of inefficiency sources [19].

Energy demand continues to rise, accompanied by increasing environmental operational limits. However, fossil fuels remain the primary energy source, with known impacts on emissions and air quality. These conditions caused continued efforts to improve engine efficiency and reduce associated environmental impacts [20, 21]. The transport sector represents a significant share of these emissions, which places engine performance optimization as a central requirement to mitigate climate change and improve air quality [22].

Previous studies considered energy and exergy behavior in diesel engines under different operating conditions [23].

Transient operation was examined using computational techniques supported by experimental validation [24]. The effects of EGR and injection timing on exergy distribution were evaluated in low-temperature combustion, and combustion-related losses were evaluated within a second-law method [25]. Fuel-related effects were also considered. Ignition delay and cetane number were linked to changes in energy and exergy performance in biodiesel operation [26]. In addition, exergy analysis was combined with emission characteristics to evaluate engine performance with vegetable oil–based fuels [27].

The influence of injection strategy and fuel combination has also been examined. An increase in injection pressure was associated with reduced energy and exergy efficiency under part-load operation [28]. Dual-fuel operation using syngas and diesel has been evaluated within a second-law formulation [29].

Combustion irreversibilities were compared across fuels, showing lower entropy generation for lighter fuels than for heavier ones [30]. Review studies have also summarized energy and exergy analyses for dual-fuel diesel engines operating on petroleum diesel and biogas [31]. In addition, exergy performance has been evaluated for microalgae biodiesel–diesel blends, together with both theoretical and experimental studies on dual-fuel operation using natural gas and diesel [32].

With the advancement of computational tools, one-dimensional engine simulation models have emerged as efficient alternatives to experimental testing. It has been demonstrated that such models provide a balance between computational cost and predictive accuracy, making them suitable for parametric studies [33]. Diesel-RK is commonly used to simulate diesel engine combustion, performance, and emissions, with results that agree with experimental data [34].

However, most simulation studies focus on performance and emissions, while exergy-based evaluation across different operating conditions remains limited. In particular, the free version of Diesel-RK does not include built-in exergy analysis capabilities, which limits its direct application for second-law evaluation.

Therefore, there is a need for an externally implemented exergy analysis framework that utilizes diesel-RK outputs to assess exergy efficiency, destruction, and distribution characteristics under realistic engine operating conditions. The present study addresses this gap by applying a combined thermal and exergy-based approach to evaluate diesel engine performance over a wide range of speed–load conditions using Diesel-RK simulation.

Accordingly, the present study aims to develop and apply a predictive exergy-based framework based on thermodynamic data extracted from Diesel-RK simulations to investigate the effect of engine load on the exergetic performance of a turbocharged diesel engine. The specific objectives are to:

(i)Simulate engine performance under different load conditions using Diesel-RK.

(ii) perform a combined thermal and exergetic assessment based on the extracted simulation data;

(iii) quantify the influence of load on fuel exergy input, useful work, exhaust losses, heat-transfer-related losses, and internal destruction; and

(iv) analyze the variation of exergetic efficiency with engine load and identify the dominant sources of irreversibility across the investigated operating conditions.

It should be noted that the exergy analysis is implemented externally using Diesel-RK simulation outputs, since the free version of the software does not directly provide exergy-related parameters.

3. METHODS AND MATERIALS

3.1 Diesel-RK model setup and engine specifications

A one-dimensional Diesel-RK engine model was developed to assess turbocharged diesel engine performance, focusing on both thermal and exergy-based metrics across different speed–load conditions. The model utilized the geometric and operating specifications of a 2.4 L MIVEC turbocharged diesel engine (4N15), as listed in Table 1. The simulations were carried out while maintaining constant boundary and ambient conditions for all cases to ensure consistent comparisons across the operating matrix.

Engine load variation was achieved by regulating the fuel injection quantity per cycle at each fixed engine speed. The thermodynamic and performance inputs needed for the energy and exergy analyses were obtained directly from Diesel-RK outputs. These included in-cylinder pressure temperature histories, air and fuel flow rates, brake power, BSFC, heat-transfer terms, and key exhaust-state properties.

The coolant heat loss was evaluated as the sum of the heat transfer rates through the cylinder head and cylinder liner. Heat transfer through the piston crown was excluded and considered part of the lubricating oil heat transfer. In Diesel-RK reports, wall heat transfer is included within the coolant heat loss and was therefore not treated as an independent loss term. Since Diesel-RK does not explicitly provide the lubricating oil and exhaust heat losses, an unaccounted heat-loss term was calculated from the overall energy balance to represent the combined effect of these unreported losses.

Table 1. Engine specifications - 2.4L MIVEC Turbo Diesel (4N15)

Engine Parameter	Specification
Number of cylinders and arrangement	4-Cylinder, 4-Stroke, In-line
Valvetrain	DOHC, 16 Valves
Combustion Chamber	Pentroof Type
Fuel System	Electronic Common Rail direct injection
Displacement (cm^3)	2,439
Bore × Stroke mm	86.0 × 105.0
Compression Ratio	15.5:1
Intake Valve Timing	IO 8° BTDC, IC 30° ABDC
Exhaust Valve Timing	EO 44° BBDC, EC 16° ATDC
Max Output	133 kW at 3500 rpm
Max Torque	430 Nm at 2500 rpm
Number of injectors per cylinder	1
Injector nozzle bore	0.16 mm
Number of nozzles	3
Ambient parameters	Pressure 1 bar, Temperature 313 K
Compressor PR	1.54

3.2 Operating matrix and load definition

The investigated operating range covered engine speeds from 1000 to 4000 rpm. For each engine speed, four load levels (25%, 50%, 75%, and 100%) were simulated by varying the injected fuel quantity per cycle. At every speed, the 100% load condition was first established by increasing the fuel quantity until the engine reached its maximum design torque. The related full-load fuel quantity was then used as a reference to determine the remaining fuel quantity for the part-load (75%, 50%, and 25%) by applying fixed fractions of the full-load value, as listed in Table 2.

Table 2. Fuel injection quantity per cycle (g/cycle) at different speeds and loads

Speed (rpm)	25% Load	50% Load	75% Load	100% Load
1000	0.01621	0.03243	0.04864	0.06485
2000	0.02019	0.04038	0.06056	0.08075
3000	0.02416	0.04833	0.07249	0.09665
4000	0.02814	0.05628	0.08441	0.11255

3.3 Model calibration procedure

The Diesel-RK model was calibrated at two reference points representing the rated engine conditions: 430 Nm at 2500 rpm and 133 kW at 3500 rpm. For the rated-torque calibration, the engine speed was set to 2500 rpm, and the injected fuel quantity was tuned until the simulated brake torque reached 430 N·m, which occurred at 0.0887 g/cycle. For the rated power calibration, the engine speed was fixed at 3500 rpm, and the injected fuel quantity was adjusted until the simulated brake power matched 133 kW, which required 0.10460 g/cycle. After completing calibration, the validated model was used to simulate the complete speed–load matrix listed in Table 2.

3.4 Thermal energy analysis

Thermal performance analysis was carried out in accordance with the first law of thermodynamics and conventional protocols for evaluating engine performance.

3.4.1 Brake thermal efficiency

The brake thermal efficiency (η_{th}) is defined as the ratio of brake power output to the chemical energy input of the fuel, representing the efficiency of converting fuel energy into useful work.

$$\eta_{\mathrm{th}} = \frac{\mathrm{BP}}{\mathrm{FP}} = \frac{\mathrm{BP}}{\dot{m}_{\mathrm{f}}\,\mathrm{LHV}} \tag{1}$$

3.4.2 Energy balance

An ICE energy balance equation measures the conversion of fuel energy into useful work (brake power), heat transferred to coolant, heat in exhaust, and other losses (friction, oil, radiation), generally stated as:

$$\dot{\mathrm{Q}}_{\mathrm{fuel}} = \mathrm{BP} + \dot{\mathrm{Q}}_{\mathrm{cooling}} + \dot{\mathrm{Q}}_{\mathrm{exh}} + \dot{\mathrm{Q}}_{\mathrm{loss}} \tag{2}$$

where, $\dot{\mathrm{Q}}_{\mathrm{fuel}}$ is the fuel energy input, BP is the brake power, $\dot{\mathrm{Q}}_{\mathrm{cooling}}$ is the heat rejected to the coolant, $\dot{\mathrm{Q}}_{\mathrm{exh}}$ is the exhaust heat, and $\dot{\mathrm{Q}}_{\mathrm{loss}}$ represents unaccounted losses such as friction, lubrication oil losses, and radiation.

3.5 Exergy analysis

Exergy analysis quantifies the loss of work potential in energy conversion systems. Energy is conserved in all processes, whereas exergy decreases due to heat transfer, mixing, and friction. Applying exergy analysis to thermal systems allows these loss mechanisms to be identified and supports the development of measures to reduce exergy destruction. In this work, exergy analysis was performed based on the second law of thermodynamics to quantify thermodynamic losses and evaluate the quality of energy conversion. The dead-state conditions were assumed as an ambient pressure of 1 bar and an ambient temperature of 313 K, consistent with the simulation boundary conditions.

3.5.1 Fuel chemical exergy

The exergy input rate to the engine due to mass transfer consisted of the chemical exergy rate of the fuel and that of the combustion air. However, the contribution of the combustion air exergy may be neglected if the air is assumed to enter the engine at ambient conditions. The specific chemical exergy of the fuel was estimated using the relation:

$$\varphi_{\mathrm{f}} = \beta.\,\mathrm{LHV} \tag{3}$$

where, φ_{f} is the specific chemical exergy of the fuel (kJ/kg), β is the fuel chemical exergy factor, typically ranging from 1.04 to 1.07 for diesel fuel, and LHV is the lower heating value of the fuel (kJ/kg). Accordingly, the fuel exergy rate is calculated as:

$$\dot{\mathrm{E}}\mathrm{x}_{\mathrm{fuel}} = \dot{m}_{\mathrm{f}}.\varphi_{\mathrm{f}} = \dot{m}_{\mathrm{f}}.\beta.\,\mathrm{LHV} \tag{4}$$

The approximation of the fuel chemical exergy factor (β) is widely accepted in exergy analyses of ICEs and was estimated using:

$$\beta = 1.0401 + 0.1728\frac{\mathrm{h}}{\mathrm{c}} + 0.0432\frac{\mathrm{o}}{\mathrm{c}} + 0.2169\frac{\alpha}{\mathrm{c}}\left(1 - 2.0628\frac{\mathrm{h}}{\mathrm{c}}\right) \tag{5}$$

where, h, c, o, and a are the mass fractions of H, C, O, and S, respectively.

3.5.2 Work exergy

The useful work exergy is assumed equal to the brake power:

$$\dot{E}x_{work} = BP \quad (6)$$

This assumption is commonly adopted in exergy-based engine performance studies.

3.5.3 Exergy associated with heat transfer

The exergy transfer with heat is calculated as:

$$\dot{E}x_{heat} = \left(1 - \frac{T_0}{T}\right) \dot{Q} \quad (7)$$

where, T_0 is the ambient temperature, and T is the boundary temperature at which heat transfer occurs. This formulation is derived from classical exergy theory. The boundary temperature T was taken as the average temperature of the corresponding heat transfer sink (coolant or oil), as reported directly by Diesel-RK outputs.

3.5.4 Exhaust gas exergy

The physical exergy of exhaust gases is expressed as:

$$\dot{E}x_{exh} = \dot{m}_{exh}[(h - h_0) - T_0(s - s_0)] \quad (8)$$

where, h and s are the specific enthalpy and entropy of the exhaust gases, and the subscript 0 denotes dead-state conditions. This approach has been extensively applied in diesel engine exergy analyses.

3.5.5 Exergy destruction

The total exergy destruction within the engine is calculated from the exergy balance:

$$\dot{E}x_{dest} = \dot{E}x_{fuel} - \left(\dot{E}x_{work} + \dot{E}x_{heat} + \dot{E}x_{exh}\right) \quad (9)$$

This equation represents the net thermodynamic losses associated with combustion, heat transfer, and frictional effects.

3.5.6 Exergy efficiency

The exergetic efficiency of the engine is defined as the ratio of useful work exergy to the fuel exergy input:

$$\eta_{ex} = \frac{\dot{E}x_{work}}{\dot{E}x_{fuel}} \quad (10)$$

This definition has been widely used in exergy performance assessments of diesel engines.

3.6 Post-processing, data screening, and external calculations

Thermal and exergy indicators were evaluated at each operating point to assess how engine load influences efficiency and loss behavior. Low-load cases showing non-physical responses were therefore omitted from the subsequent analysis. The external exergy post-processing was implemented using Excel spreadsheets, where heat transfer terms and exergy components were calculated using the extracted Diesel-RK results and the adopted thermodynamic relations.

A complete set of raw engine operating parameters, including fuel quantity, brake power, torque, mass flow rates, and intake/exhaust conditions, is provided in Appendix A (Table A1). The corresponding externally calculated exergy terms, efficiencies, and distribution fractions are reported in Appendix A (Table A2).

3.7 Physical validation of the simulation results

The physical consistency of the Diesel-RK simulation results was assessed by examining the resulting torque and brake power trends over the investigated speed–load range. The simulated torque curve followed the expected diesel-engine trend. Torque increased with both load and engine speed, reached its maximum at mid-range speeds, and then declined at higher speeds as friction and combustion losses became more significant. Brake power increased with speed and load, and its maximum value occurred at a higher engine speed more than the peak-torque point, which matches with the basic torque–speed–power relationship.

These characteristics agree with established engine theory and previously published experimental behavior, confirming that the simulated dataset is physically consistent and suitable for the thermal and exergy evaluations presented in the Results and Discussion section.

3.8 Model limitations and scope of applicability

The present study is based on a one-dimensional Diesel-RK simulation model with fixed boundary conditions, including intake pressure, ambient temperature, and fuel properties. These assumptions were adopted to isolate the effects of load and speed on exergy behavior and to maintain consistent comparisons across the operating matrix.

However, real engine operation may involve variations in intake conditions, fuel characteristics, and transient effects, which are not captured in the present model. In addition, the use of a one-dimensional approach inherently limits the resolution of in-cylinder spatial variations and detailed turbulence–chemistry interactions.

Therefore, the results of this study should be interpreted within the context of steady-state and controlled boundary conditions. The results are intended for comparative analysis and trend identification across speed–load conditions, rather than for direct quantitative prediction under all operating scenarios. Variations in intake pressure, fuel composition, and transient operation can affect the absolute values of exergy-related parameters.

Future work may extend the present framework by incorporating variable boundary conditions and advanced multi-dimensional modeling approaches to improve predictive capability under realistic engine operation.

4. RESULTS AND DISCUSSIONS

This section presents and discusses the effects of engine load on the exergy performance of the diesel engine under different operating conditions. The analysis focuses on distribution characteristics, thermodynamic losses, and exergetic efficiency.

4.1 Effect of engine load on exergy distribution

To facilitate a detailed discussion of the effect of load and speed on thermodynamic performance, the numerical values of the exergy distribution in terms of work exergy, exergy exhaust rate, exergy rate for heat transfer, and exergy destruction are first summarized in Appendix A (Table A2). The influence of engine load and engine speed is then discussed separately in the following sections.

4.1.1 Exergy distribution at 1000 rpm

Figure 1 shows the exergy distribution at 1000 rpm under different engine load conditions. At 25% load, the fuel exergy converted into useful work reaches about 7.07%, while 3.70% is related to the heat transfer, 41.16% is carried by the exhaust gas, and finally, 48.07% is lost through internal destruction. This behavior is associated with increased thermodynamic losses, particularly heat transfer at low load. At 50% and 75% engine load, the work exergy increased considerably from 15.66% to 27.25%. The reduction in the heat transfer losses from 3.67% to 3.38% reflected a decrease in the thermal loss fraction under increasing load. At full load, the work exergy reached 31.93%, while heat transfer losses reduced further to 3.18%. Exergy destruction remained the major loss mechanism through all load conditions, varying between 48.07% and 43.91%, indicating significant irreversibility within the system. Increasing load at low engine speeds was associated with improved thermodynamic performance, as a larger fraction of the fuel exergy was converted into useful work.

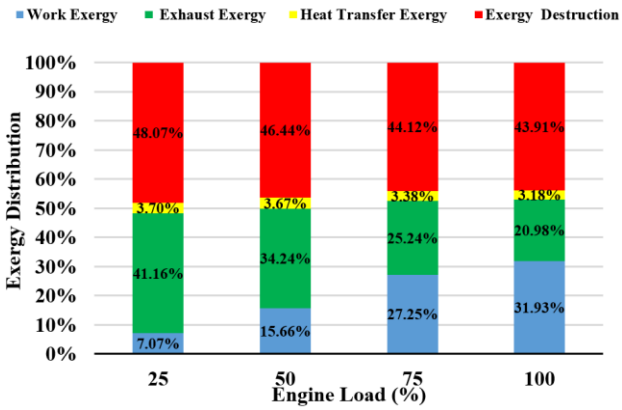

Figure 1. Exergy distribution at different loads (1000 rpm)

4.1.2 Exergy distribution at 2000 rpm

Figure 2 shows the exergy distribution at 2000 rpm under different engine load conditions. At 25% load, about 5.34% of the fuel exergy is converted into useful work, while about 2.83% is related to heat transfer; the maximum losses occur in the exhaust gases, which reached 47.22%, and 44.62% is lost through internal destruction such as friction. As the load increases to 50% and 75%, the work exergy rises from 22.44% to 32.35%, accompanied by a reduction in heat transfer-related losses from 2.53% to 2.32%. The observed distribution reflects a reduction in the relative heat loss fraction rather than a direct measure of combustion quality. At full load (100%), work exergy reached 35.12%, compared with the 75% load case, while heat transfer losses were 2.19%. Exergy destruction remained the predominant term across all load conditions, confined to 44.62–40.97%. At 2000 rpm, the exergy distribution was characterized by a higher work fraction and a lower relative heat transfer contribution.

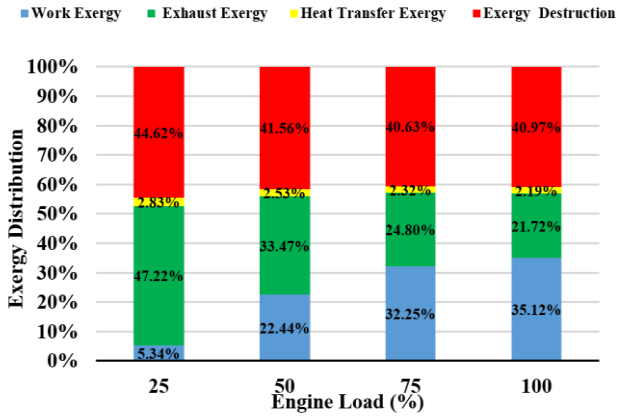

Figure 2. Exergy distribution at different loads (2000 rpm)

4.1.3 Exergy distribution at 3000 rpm

Figure 3 shows the exergy distribution at 3000 rpm at different load conditions. At 25% engine load, 11.62% of the fuel exergy is converted into useful work, while 2.37% is related to the heat transfer, 41.28% is carried by the exhaust, and 44.73% is lost through internal destruction. At 50% and 75% load, work exergy reached 32.33% and 34.80%, while heat transfer losses were 1.95–1.83%. At full load (100%), work exergy was 32.72%, with heat transfer losses at 1.87%. Exergy destruction remained within 44.73–42.56% at 3000 rpm. Higher load corresponded to higher work exergy fractions and lower relative heat transfer contributions.

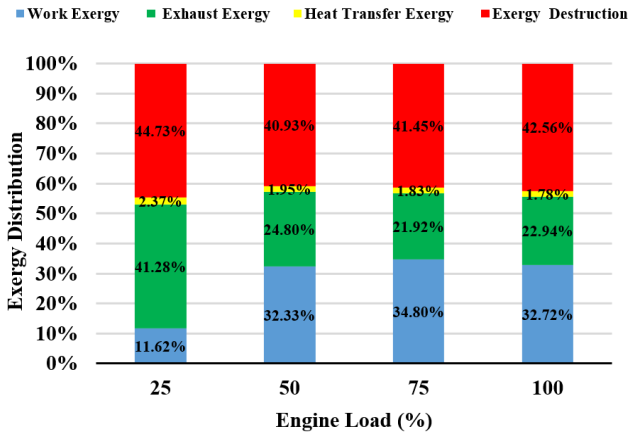

Figure 3. Exergy distribution at different loads (3000 rpm)

4.1.4 Exergy distribution at 4000 rpm

Figure 4 shows the exergy distribution at 4000 rpm under different load conditions. At 25% load, 17.53% of the fuel exergy is converted into useful work, while 1.69% is associated with heat transfer, 47.39% is carried by the exhaust, and 33.39% is lost through internal destruction. As the load increases to 50%, the work exergy rises to 29.87%, while heat transfer losses decrease to 1.63%, indicating improved energy utilization. At 75% load, the work exergy decreases to 26.93%, while heat transfer losses are approximately 1.66%. At full load (100%), the work exergy decreases to approximately 20.59%, while heat transfer losses decrease to about 1.40%. Exergy destruction increases noticeably with load, reaching a maximum value of about 53.91% at full load, reflecting intensified entropy generation under high-speed operation.

The increase in exergy destruction at high engine speeds is associated with intensified combustion rates and steeper temperature gradients, which enhance entropy generation. In addition, increased frictional losses and reduced time available for heat transfer and gas exchange further contribute to thermodynamic losses. Overall, the results at 4000 rpm indicate that although increasing load improves work exergy at intermediate loads, high engine speed shifts the system toward loss-dominated behavior, limiting overall thermodynamic performance.

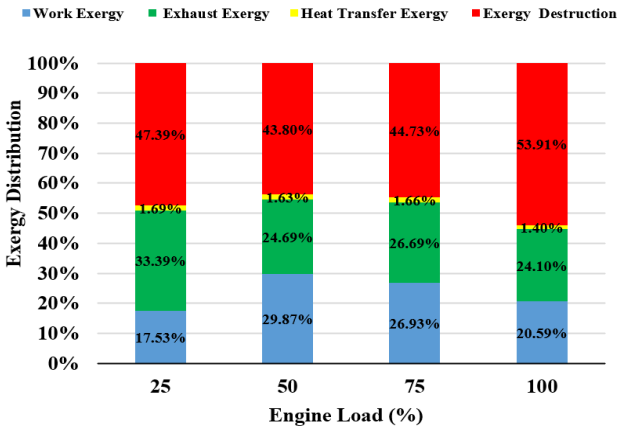

Figure 4. Exergy distribution at different loads (4000 rpm)

4.1.5 Comparative discussion of exergy distribution at different engine speeds

Figures 1–4 compare the exergy distribution across different loads and engine speeds ranging from 1000 to 4000 rpm. At 1000 and 2000 rpm, increasing load leads to a significant rise in the work exergy, reaching approximately 31.93% and 35.17% at full load, respectively, while heat transfer losses decrease to about 2.19%. This behavior reflects improved combustion effectiveness and reduced relative heat losses under higher load conditions.

At 3000 rpm, the work exergy fraction remains relatively high across medium and high loads (32–35%), indicating near-optimal thermodynamic performance. In contrast, at high speed (4000 rpm), although the work fraction improves at intermediate loads, it decreases to about 20.6% at full load, accompanied by a substantial increase in exergy destruction to approximately 53.91%. This trend is associated with intensified combustion rates, steeper temperature gradients, and increased frictional losses, which collectively enhance entropy generation and limit useful work extraction.

Furthermore, a considerable portion of the input exergy is carried away by exhaust gases, indicating incomplete recovery of high-temperature energy and highlighting the potential for waste heat recovery. Overall, these results demonstrate that moderate engine speeds combined with high loads provide the most favorable exergy distribution, whereas high-speed operation increases thermodynamic losses and constrains overall performance.

4.2 Effect of engine load and speed on exergy efficiency

Figure 5 and Appendix A (Table A2) show the variation of exergy efficiency (η_{ex}) with load and engine speed. At 1000 and 2000 rpm, η_{ex} increases monotonically with load, rising from 7.1% to 31.9% at 1000 rpm and from 5.3% to 35.1% at 2000 rpm, indicating improved utilization of fuel exergy at higher loads. At 3000 rpm and 75% load, η_{ex} reaches a maximum value of 34.8%, while at full load it slightly decreases to 32.7%, reflecting increased thermodynamic losses under high-speed, full-load conditions. A non-monotonic trend is observed at 4000 rpm, where η_{ex} increases to 29.9% at 50% load but decreases significantly to 20.6% at full load. This behavior is characteristic of a high-speed, full-load operating regime, where friction-related losses and exhaust penalties rise sharply, and the reduced time available for gas exchange and combustion intensifies entropy generation, leading to higher exergy destruction and lower η_{ex}. The results indicate that engine speeds of 2000–3000 rpm combined with high loads provide the most favorable conditions for achieving high exergy efficiency.

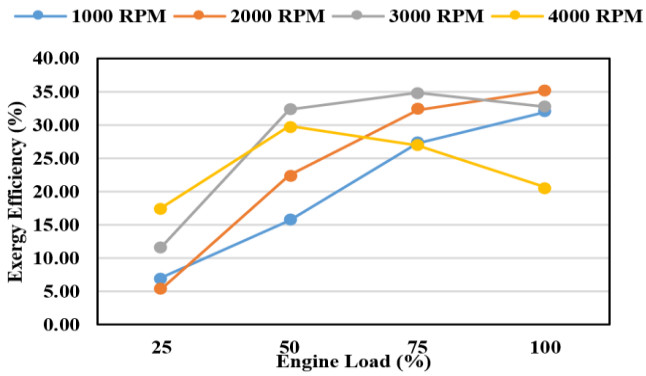

Figure 5. Effect of speed and load on diesel-engine exergy efficiency

4.3 Effect of engine load and speed on exergy destruction

Figure 6 and Appendix A (Table A2) present the variation of exergy destruction across different engine speeds. Exergy destruction increases monotonically with load at all speeds due to higher fuel input and intensified combustion and heat transfer processes. At higher loads, the increased fuel input leads to higher in-cylinder temperatures and pressure levels, which intensify heat transfer across finite temperature differences and promote entropy generation.

At 1000 rpm, exergy destruction rises from 19 kW at 25% load to 43 kW at full load, whereas at 2000 and 3000 rpm, it increases more rapidly, reaching 80 kW and 185 kW, respectively. At 4000 rpm, exergy destruction increases from 80 kW at low load to 364 kW at full load, as high-speed, high-load operation intensifies combustion-related losses.

During full load, higher fuel injection rates and faster combustion result in steeper temperature and pressure gradients, higher frictional losses, and enhanced heat transfer to the cylinder walls, all of which increase entropy generation and, consequently, exergy destruction. Overall, the results indicate that engine speed has a stronger influence on thermodynamic losses than load, particularly under full-load conditions.

To further interpret the observed trends, the increase in exergy destruction can be attributed to a combination of combustion losses, heat transfer across finite temperature differences, and mechanical friction. At higher engine speeds, rapid combustion and limited residence time lead to incomplete thermodynamic equilibration, while at higher loads, elevated temperature gradients enhance entropy generation. These mechanisms collectively govern the redistribution of fuel exergy and explain the observed

variations in exergy performance.

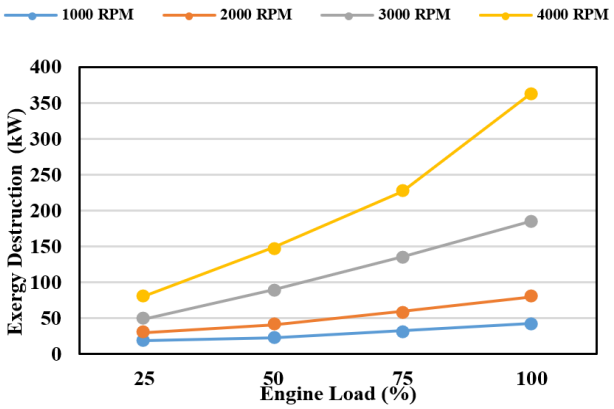

Figure 6. Effect of engine load and speed on exergy destruction of the diesel engine

4.4 Comparison of the present work with previous experimental studies

For validation, the Diesel-RK simulation results were compared with experimental data reported in the literature. Three experimental studies on diesel engine exergy analysis were selected for comparison under full-load conditions. Appendix A (Table A4) presents the comparison between the current study and previous studies in the same field [35-37].

As shown in Table A4, the work fraction and exergetic efficiency show good agreement with the experimental results. This agreement can be attributed to consistent thermodynamic trends governing diesel engine operation, particularly the dominant role of combustion-related losses and heat transfer in determining overall thermodynamic losses. Despite differences in engine configurations and fuels, these mechanisms lead to comparable distribution trends.

Except at 4000 rpm, the predicted work fraction and exergetic efficiency are within ±7% of the experimental data. The remaining deviations may be related to differences in engine type, operating conditions, and fuel properties, which influence combustion characteristics, in-cylinder temperature levels, and exhaust energy distribution, thereby affecting the magnitude of the calculated components. In addition, the simplified assumptions of the one-dimensional model may contribute to these discrepancies, particularly at high engine speeds.

Overall, the present results are within ±5% of the experimental values, confirming a good level of agreement. From a practical perspective, this comparison demonstrates that the Diesel-RK-based framework provides reliable estimates of thermodynamic performance under controlled conditions, supporting its use as a cost-effective alternative to experimental analysis for performance evaluation and preliminary optimization studies.

In addition, unlike most previous studies that rely on direct experimental measurements or advanced simulation tools, the present work demonstrates that externally implemented exergy analysis based on one-dimensional simulation outputs can effectively capture the main thermodynamic trends and dominant loss mechanisms.

From an operational perspective, the results indicate that moderate engine speeds combined with high load conditions provide the most favorable performance, while high-speed operation under full load should be avoided due to increased thermodynamic losses. These findings can support engine calibration and optimization of operating conditions in practical diesel engine applications.

While previous studies have primarily relied on experimental investigations or advanced simulation tools with built-in exergy capabilities, the present study differs by implementing an external exergy analysis framework based on Diesel-RK outputs. This approach enables systematic evaluation of exergetic efficiency, destruction, and distribution characteristics under controlled variable load and speed conditions using a computationally efficient one-dimensional model.

In addition, the present work provides a consistent mapping of thermodynamic behavior across a wide operating range, offering both thermodynamic insight and practical guidance for engine performance optimization. This combination of methodological simplicity, predictive capability, and operational relevance distinguishes the current study from existing literature.

4.5 Implications of the present study for energy sustainability

The results demonstrate that thermal and exergy analysis play a key role in enhancing the sustainability of diesel engine operation. By analyzing the distribution of fuel chemical exergy into useful work, exhaust losses, heat transfer, and internal losses, the study emphasizes energy quality rather than quantity. Increasing load enhances the conversion of fuel exergy into useful work while reducing thermodynamic losses, thereby reducing fuel consumption and resource wastage. The substantial exergy carried by exhaust gases highlights the potential of waste heat recovery systems to enhance overall efficiency and reduce fuel consumption. Exergy-based performance assessment supports long-term energy efficiency by guiding the selection of optimal operating conditions for improved efficiency and sustainability.

4.6 Regression-based modeling of exergy efficiency and destruction

To enhance the practical applicability of the results, mathematical models were developed to predict exergetic efficiency and destruction rate. The models were based on engine speed, injected fuel quantity per cycle, and excess air ratio, which represent the main operating and combustion-related parameters. A linear model with interaction terms was sufficient to describe efficiency, whereas the destruction rate required a logarithmic formulation due to its nonlinear trend at higher operating conditions. The model coefficients were obtained using least-squares regression applied to Diesel-RK simulation data. The predicted values were compared with the simulation data, showing good agreement across the studied operating conditions.

The scaled variable n was obtained from the engine speed N using the linear transformation in Eq. (11), where N is expressed in rpm. This scaling does not introduce a new physical parameter; it is used only to facilitate the regression analysis. Efficiency and destruction rate were then correlated as functions of the scaled variable n, the injected fuel quantity per cycle ($\dot{m}_f$), and the excess air ratio (λ), as expressed in Eqs. (12) and (13). The injected fuel quantity was used as a direct indicator of engine load.

$$n = \frac{N\ (rpm)}{1000} \tag{11}$$

$$\begin{aligned}\eta_{ex}(\%) = {} & 6.6213 + 16.84\ n + 404.24\ \dot{m}_f \\ & - 0.936\ \lambda - 1.08\ n^2 \\ & - 157.9\ (n.\dot{m}_f) - 0.88\ (n\ \lambda) \\ & - 626.47(\dot{m}_f)^2 + 24.54\ (\dot{m}_f.\lambda) \\ & - 0.795\ \lambda^2\end{aligned} \tag{12}$$

$$\begin{aligned}\ln\left(\dot{Q}_{dest}(kW)\right) = {} & 2.81 + 0.0.59\ n + 12.69\ \dot{m}_f \\ & - 0.279\ \lambda - 0.0136\ n^2 \\ & - 0.67\ (n.\dot{m}_f) - 0.0037\ (n\ \lambda) \\ & - \ 6.25(\dot{m}_f)^2 - 1.93\ (\dot{m}_f.\lambda) \\ & - 0.014\ \lambda^2\end{aligned} \tag{13}$$

The quadratic regression model predicted η_{ex} with high accuracy ($R^2 = 0.9907$, RMSE ≈ 0.93 percentage points) over the investigated operating matrix. In addition, the $\dot{Q}_{dest}$ model achieved an excellent fit ($R^2 = 0.99965$, RMSE ≈ 0.0159 in the log domain). The predicted values were compared with the simulation data and showed close agreement across the studied speed–load conditions. The comparison is presented in Appendix A (Table A3). The relatively higher deviations in the predicted efficiency at some operating points are primarily associated with light-load conditions, where the actual values are inherently low. Consequently, even small absolute differences can lead to relatively large percentage deviations.

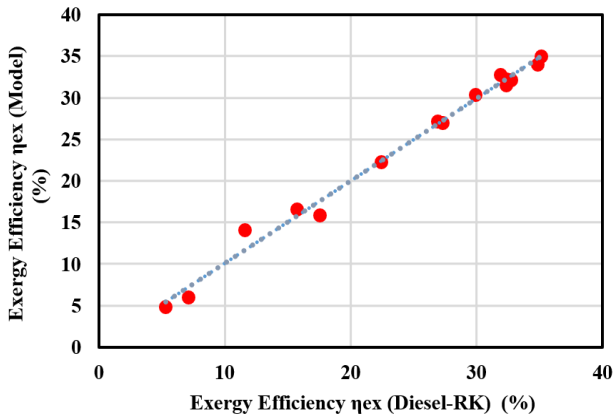

Figure 7. Comparison of exergy efficiency predicted by the mathematical model and calculated using Diesel-RK

Figure 7 compares the predicted exergy efficiency with the corresponding Diesel-RK results across all operating conditions. The diagonal 1:1 line is included as a reference for perfect agreement. Deviations above and below the line represent slight overestimation and underestimation, respectively. Overall, the data remain close to the parity line, indicating that the model accurately captures the variation of exergy efficiency across the investigated speed–load range.

Figure 8 compares the predicted destruction rate with the corresponding Diesel-RK results across all operating conditions. The diagonal 1:1 line is included as a reference for perfect agreement. The results remain close to the parity line, indicating that the model reproduces the Diesel-RK predictions with good accuracy across the speed–load range. Small deviations occur at a few conditions, particularly at high speed and high load, where the behavior becomes increasingly nonlinear. Overall, the model provides a consistent and reliable prediction of $\dot{Q}_{dest}$.

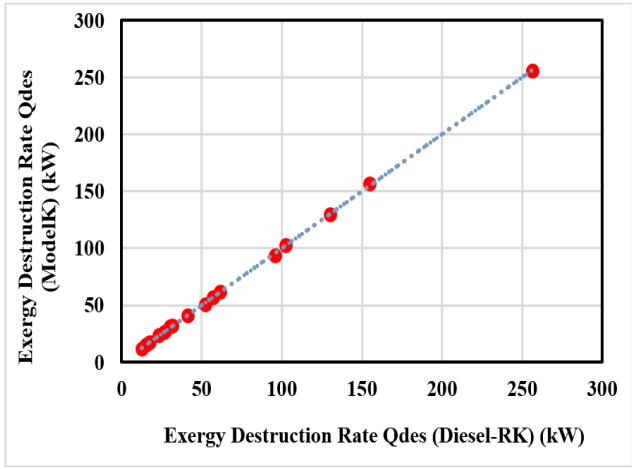

Figure 8. Comparison of exergy destruction predicted by the mathematical model and calculated using Diesel-RK

From an operational perspective, optimal performance is achieved at moderate speeds and high loads, while high-speed operation under full load leads to increased thermodynamic losses. These findings support engine calibration and optimization of operating conditions in practical diesel engine applications.

5. CONCLUSION

This study presents a combined thermal and exergy-based analysis of a turbocharged diesel engine operating under variable load and speed conditions using Diesel-RK simulation, providing insight beyond conventional first-law analysis. The collected results showed that:

1. At low and moderate speeds, exergy efficiency increases with the increase of load and reaches its maximum value of approximately 35.1% at 2000 rpm and full load, indicating optimal operating conditions.
2. At high speed (4000 rpm), exergy efficiency decreases to about 20.6% at full load due to intensified thermodynamic losses.
3. Exergy destruction increases significantly with both the increase of load and speed, where it rises from about 19 kW at low load to nearly 364 kW at high-speed full-load operation, highlighting the dominant effect of speed on entropy generation. The distribution trends indicate that moderate speeds combined with high loads provide the most favorable performance, characterized by higher work fractions and reduced relative losses.
4. These findings highlight the importance of load–speed optimization for improving efficiency and reducing losses. Operation at moderate speeds (2000–3000 rpm) and high loads improves performance, whereas high-speed full-load operation leads to significant penalties.
5. Based on the collected results from this work, control strategies are required at moderate-speed, high-load regimes. In addition, the significant exhaust energy losses highlight the potential for waste heat recovery systems.
6. Since fuel type is expected to influence exergy distribution due to variations in chemical composition and combustion characteristics, future work may extend this framework to assess the effect of fuel composition on loss mechanisms under varying operating conditions.

ACKNOWLEDGMENT

The author acknowledges the Deanship of Scientific Research, Qassim University, for supporting this research. Finally, thanks to Professor Andrey Kuleshov (Moscow State Technical University) for allowing us to use the Diesel- RK.

REFERENCES

[1] Bayramoğlu, K. (2024). Energy and exergy analysis of diesel-hydrogen and diesel-ammonia fuel blends in diesel engine. Journal of ETA Maritime Science, 12(2): 128-135. https://doi.org/10.4274/jems.2024.46503

[2] Dahham, R.Y., Wei, H., Pan, J. (2022). Improving thermal efficiency of internal combustion engines: Recent progress and remaining challenges. Energies, 15(17): 6222. https://doi.org/10.3390/en15176222

[3] Costea, M., Petrescu, S., Feidt, M., Dobre, C., Borcila, B. (2021). Optimization modeling of irreversible Carnot engine from the perspective of combining finite speed and finite time analysis. Entropy, 23(5): 504. https://doi.org/10.3390/e23050504

[4] Paloboran, M., Darmawang, D., Pagasis, T., Atarezcha, P. (2026). Thermodynamics analysis to evaluate the combustion process of E50 fuel with injection volume variation. Journal of Applied Engineering Science, 24(1): 130–143. https://doi.org/10.5937/jaes0-55123

[5] Nanadegani, F.S., Sunden, B. (2023). Review of exergy and energy analysis of fuel cells. International Journal of Hydrogen Energy, 48(84): 32875-32942. https://doi.org/10.1016/j.ijhydene.2023.05.052

[6] Bayramoğlu, K., Nuran, M. (2023). Energy, exergy, sustainability evaluation of the usage of pyrolytic oil and conventional fuels in diesel engines. Process Safety and Environmental Protection, 181: 324-333. https://doi.org/10.1016/j.psep.2023.11.034

[7] Doğan, B., Erol, D. (2022). The investigation of energy and exergy analyses in compression ignition engines using diesel/biodiesel fuel blends-a review. Journal of Thermal Analysis and Calorimetry, 148(5): 1765-1782. https://doi.org/10.1007/s10973-022-11862-y

[8] Agrebi, S., Dreßler, L., Nishad, K. (2022). The exergy losses analysis in adiabatic combustion systems including the exhaust gas exergy. Entropy, 24(4): 564. https://doi.org/10.3390/e24040564

[9] Mohammed, H.N., Imran, M.S., Kurji, H.J. (2024). Energy and exergy analysis of thermoelectric generator installed on diesel engine exhaust heat recovery system. International Journal of Heat and Technology, 42(6): 420624. https://doi.org/10.18280/ijht.420624

[10] Tiwari, C., Verma, T.N., Dwivedi, G., Verma, P. (2023). Energy-exergy analysis of diesel engine fueled with microalgae biodiesel-diesel blend. Applied Sciences, 13(3): 1857. https://doi.org/10.3390/app13031857

[11] Raja, S., Kumar, M.S., Natarajan, S., Eshwar, D., Alphin, M. (2022). Energy and exergy analysis and multi-objective optimization of a biodiesel fueled direct ignition engine. Results in Chemistry, 4: 100284. https://doi.org/10.1016/j.rechem.2022.100284

[12] Sayyed, S., Das, R.K., Kulkarni, K. (2022). Energy and exergy analyses of multiple biodiesel blended diesel engine. Journal of Energy Resources Technology, 145(4): 1-26. https://doi.org/10.1115/1.4054850

[13] Gnanamani, S., Gaikwad, P.U., Subramaniam, L., Chandralingam, R. (2022). Exergy analysis in diesel engine with binary blends. Thermal Science, 26(1 Part A): 353-362. https://doi.org/10.2298/tsci200808273g

[14] Thanh, N.C., El Askary, A., Elfasakhany, A., Nithya, S. (2021). Exergy and energy analyses of the spirulina microalgae blends in a direct injection engine at variable engine loads. Journal of Energy Resources Technology, 143(12): 405180. https://doi.org/10.1115/1.4052180

[15] Li, B. (2025). Thermodynamic limits and chemical energy conversion efficiency in internal combustion engines. Science and Technology of Engineering, Chemistry and Environmental Protection, 1(5): 1-5. https://doi.org/10.61173/cngxkz55

[16] Erol, D., Yeşilyurt, M.K., Yaman, H., Doğan, B. (2022). Evaluation of the use of diesel-biodiesel-hexanol fuel blends in diesel engines with exergy analysis and sustainability index. Fuel, 337: 126892. https://doi.org/10.1016/j.fuel.2022.126892

[17] Çengel, Y.A., Kanoğlu, M. (2025). Exergy efficiency of closed and unsteady-flow systems. Entropy, 27(9): 943. https://doi.org/10.3390/e27090943

[18] Feliciano, H.N.F., Rovai, F.F., Mady, C.E.K. (2023). Energy, exergy, and emissions analyses of internal combustion engines and battery electric vehicles for the brazilian energy mix. Energies, 16(17): 6320. https://doi.org/10.3390/en16176320

[19] Feng, H., Chen, X., Sun, L., Ma, R., Zhang, X., Zhu, L., Yang, C. (2023). The effect of methanol/diesel fuel blends with co-solvent on diesel engine combustion based on experiment and exergy analysis. Energy, 282: 128792. https://doi.org/10.1016/j.energy.2023.128792

[20] Emmanuel, J.K., Ngabala, F.J. (2026). Global energy demand and the role of technological innovation towards renewable energy generation for economic growth and a cleaner environment: A review. Sustainable Environment, 12(1): 2633481. https://doi.org/10.1080/27658511.2026.2633481

[21] Liu, W. (2021). Energy consumption analysis and comprehensive energy efficiency evaluation of campus central heating system based on heat supply monitoring platform. International Journal of Heat and Technology, 39(3): 746-754. https://doi.org/10.18280/ijht.390308

[22] Kováčiková, K., Novák, A., Sedláčková, A.N., Kováčiková, M. (2024). The environmental consequences of engine emissions in air and road transport. Atmosphere, 15(8): 903. https://doi.org/10.3390/atmos15080903

[23] Gupta, K., Singh, N., Goswami, P., Priyam, A. (2025). Energy and exergy analysis of diesel engine fuelled with hydrogen and Algae Oil as secondary fields. International Journal of Hydrogen Energy, 163: 150712. https://doi.org/10.1016/j.ijhydene.2025.150712

[24] Levchenko, D., Grytsyuk, O., Tsiuman, M., Yakovlieva, A. (2025). Experimental and computational optimization of cold-start performance in 4DTNA series diesel engines under variable environmental conditions. ASEAN Journal of Science and Engineering, 5(3): 559-578. https://doi.org/10.17509/ajse.v5i3.89104

[25] Krishnamoorthy, A., Ganesan, N. (2025). Energy, exergo-economic, sustainability, and combustion analysis of a dual-fuel diesel engine operating with hydrogen fuel. International Journal of Hydrogen Energy, 142: 269-291.

https://doi.org/10.1016/j.ijhydene.2025.05.419
[26] Vargün, M., Yılmaz, I.T., Özsezen, A.N., Sayın, C. (2025). A study on combustion parameters and exhaust characteristics in a diesel engine using alternative fuels at different SOI and GPP. Processes, 13(9): 3024. https://doi.org/10.3390/pr13093024
[27] Momin, G.G., Jain, N.L., Kumar, B. (2024). The performance and emission analysis of a diesel engine using vegetable oil blends and bio-diesel as fuel - A review. Journal of Mines, Metals and Fuels, 72(2): 637–650. https://doi.org/10.18311/jmmf/2024/45150
[28] Kishore, K., Pradeep, P., Mittal, M. (2026). Experimental and simulation study of advanced injection strategies in an ammonia-diesel dual-fuel engine for performance and combustion evaluation. Scientific Reports. https://doi.org/10.1038/s41598-026-49110-0
[29] Diané, A., Yomi, G.W., Zongo, S., Daho, T., Jeanmart, H. (2023). Characterization, at partial loads, of the combustion and emissions of a dual-fuel engine burning diesel and a lean gas surrogate. Energies, 16(15): 5587. https://doi.org/10.3390/en16155587
[30] Gheraissa, N., Bouras, F., Khaldi, F., Hidouri, A., Agrebi, S., Chrigui, M., Dogga, A. (2024). Comparative study of combustion processes generated by the use of different fuels: energy and exergy analysis. Combustion Theory and Modelling, 28(5): 579–605. https://doi.org/10.1080/13647830.2024.2357613
[31] Ai, W., Cho, H.M. (2025). The effects of Biosyngas and biogas on the operation of dual-fuel diesel engines: A review. Energies, 18(21): 5810. https://doi.org/10.3390/en18215810
[32] Şanli, B.G. (2019). Energetic and exergetic performance of a diesel engine fueled with diesel and microalgae biodiesel. Energy Sources, Part A: Recovery, Utilization, and Environmental Effects, 41(20): 2519–2533. https://doi.org/10.1080/15567036.2019.1587097
[33] Marinoni, A., Tamborski, M., Cerri, T., Montenegro, G., D'errico, G., Onorati, A., Piatti, E., Pisoni, E.E. (2021). 0D/1D thermo-fluid dynamic modeling tools for the simulation of driving cycles and the optimization of IC engine performances and emissions. Applied Sciences, 11(17): 8125. https://doi.org/10.3390/app11178125
[34] Rehman, M., Kesharvani, S., Dwivedi, G. (2023). Numerical investigation of performance, combustion, and emission characteristics of various microalgae biodiesel on CI engine. Fuels, 4(2): 132-155. https://doi.org/10.3390/fuels4020009
[35] Kul, B.S., Kahraman, A. (2016). Energy and exergy analyses of a diesel engine fuelled with biodiesel-diesel blends containing 5% bioethanol. Entropy, 18(11): 387. https://doi.org/10.3390/e18110387
[36] Tiwari, C., Verma, T.N., Dwivedi, G., Verma, P. (2023). Energy-exergy analysis of diesel engine fueled with microalgae biodiesel-diesel blend. Applied Sciences, 13(3): 1857. https://doi.org/10.3390/app13031857
[37] Al-Najem, N., Diab, J. (1992). Energy-exergy analysis of a diesel engine. Heat Recovery Systems and CHP, 12(6): 525-529. https://doi.org/10.1016/0890-4332(92)90021-9

NOMENCLATURE

BP	brake power, kW
BTE	brake thermal efficiency, %
BSFC	brake specific fuel consumption, g·kWh^{-1}
$\dot{E}_{fuel}$	fuel energy rate, kW
$\dot{E}x_{dest}$	exergy destruction rate, kW
$\dot{E}x_{exh}$	exhaust exergy rate, kW
$\dot{E}x_{fuel}$	fuel chemical exergy rate, kW
$\dot{E}x_{heat}$	exergy rate associated with heat losses, kW
LHV	lower heating value, MJ·kg^{-1}
$\dot{m}_{air}$	air mass flow rate, kg. s^{-1}
$\dot{m}_{d}$	diesel mass flow rate, kg. s^{-1}
$\dot{m}_{exh}$	exhaust mass flow rate, kg. s^{-1}
$\dot{m}_{f}$	total fuel mass flow rate, kg. s^{-1}
$\dot{m}_{H2}$	hydrogen mass flow rate, kg. s^{-1}
N	engine speed, rpm
p	pressure, kPa
T	temperature, K
T_0	reference (dead-state) temperature, K

Greek symbols

η_{ex}	exergy efficiency, %
λ	excess-air ratio
ϕ	chemical exergy factor

Subscripts

0	reference (dead state)
d	diesel
dest	destruction
exh	exhaust
f	fuel
H_2	hydrogen
heat	heat loss

APPENDIX A

Table A1. Raw engine operating data obtained from Diesel-RK simulations at different engine speeds and load conditions

Case ID	Speed (rpm)	Load (%)	Fuel qty (g/cycle)	Brake Torque (N.m)	Brake Power (kW)	BMEP (bar)	BSFC (g/kWh)	Brake Thermal eff. (%)	Air mass Flow (kg/h)	Fuel Mass Flow (kg/h)	λ (Lambda)	Intake T (K)	Intake p (bar abs)	Exhaust T (K)	Exhaust p (bar abs)
1	1000	25	0.0264	26.749	2.801	1.3777	1131	7.489	194.328	3.16793	4.233	367.56	3.03	646.27	7.45
2	1000	50	0.03243	72.816	7.6247	3.7503	510.4	16.596	195.48	3.89165	3.466	367.23	3.03	663.37	6.96
3	1000	75	0.04864	190.11	19.907	9.7916	293.2	28.89	198.864	5.83673	2.351	366.27	3.03	734.85	5.56
4	1000	100	0.06485	296.94	31.093	15.293	250.28	33.844	201.672	7.78196	1.788	364.32	3.03	808.28	4.39
5	2000	25	0.0219	16.756	3.5091	0.86301	1497.8	5.655	396.432	5.25593	5.204	362.68	3.02	627.42	6.78
6	2000	50	0.03243	104.36	21.856	5.3751	356.11	23.786	402.192	7.78314	3.565	361.85	3.02	666.75	5.77
7	2000	75	0.04864	224.98	47.116	11.587	247.76	34.188	408.132	11.67346	2.412	360.40	3.02	740.41	4.59
8	2000	100	0.06485	326.61	68.4	16.822	227.54	37.226	414.396	15.56374	1.837	358.36	3.02	835.84	3.69
9	3000	25	0.02416	40.276	12.652	2.0744	687.43	12.322	588.132	8.69736	4.666	361.82	3.00	639.94	5.78

10	3000	50	0.04833	224.04	70.38	11.539	247.21	34.264	605.664	17.39864	2.402	359.10	3.00	759.90	4.05
11	3000	75	0.07249	361.77	113.64	18.633	229.63	36.888	618.264	26.09515	1.635	357.05	3.00	926.76	2.99
12	3000	100	0.09665	453.48	142.46	23.356	244.24	34.681	624.636	34.79443	1.239	356.99	3.00	1144.20	2.36
13	4000	25	0.02814	70.743	29.631	3.6436	455.85	18.582	671.4	13.50729	3.430	364.14	2.99	729.45	4.24
14	4000	50	0.05628	241.07	100.97	12.416	267.54	31.661	700.2	27.01351	1.788	359.49	2.97	950.68	2.86
15	4000	75	0.08441	325.94	136.52	16.787	296.78	28.542	717.48	40.51641	1.222	357.76	2.98	1274.00	2.15
16	4000	100	0.11255	332.35	139.21	17.118	388.09	21.827	719.712	54.02601	0.919	357.72	2.98	1421.10	1.95

Table A2. Percentage distribution of (fuel exergy into work exergy, heat transfer related exergy, and exergy destruction), exergy efficiency, and exergy destruction at different engine loads and speeds

Engine Speed rpm	Load (%)	Work Exergy (%)	Exhaust Exergy (%)	Exergy of Heat Transfer (%)	Exergy Destruction (%)	Exergy efficiency (%)	Exergy destruction (kW)
1000	25	7.07	41.16	3.70	48.07	7.07	19
	50	15.66	34.24	3.67	46.44	15.66	23
	75	27.25	25.24	3.38	44.12	27.25	32
	100	31.93	20.98	3.18	43.91	31.93	43
2000	25	5.34	47.22	2.83	44.62	5.34	29
	50	22.44	33.47	2.53	41.56	22.44	40
	75	32.25	24.80	2.32	40.63	32.25	59
	100	35.12	21.72	2.19	40.97	35.12	80
3000	25	11.62	41.28	2.37	44.73	11.62	49
	50	32.33	24.80	1.95	40.93	32.33	89
	75	34.80	21.92	1.83	41.45	34.80	135
	100	32.72	22.94	1.78	42.56	32.72	185
4000	25	17.53	33.39	1.69	47.39	17.53	80
	50	29.87	24.69	1.63	43.80	29.87	148
	75	26.93	26.69	1.66	44.73	26.93	227
	100	20.59	24.10	1.40	53.91	20.6	364

Table A3. Detailed comparison of predicted and simulated exergy efficiency and exergy destruction with relative error

N (rpm)	n = N/1000	Load (%)	$\dot{m}_f$ g/cycle	λ	η_{ex}(%) Act.	$\dot{Q}_{dest}$(kW) Act.	η_{ex}(%) Pred.	ln ($\dot{Q}_{dest}$(kW)) Pred.	($\dot{Q}_{dest}$(kW)) Pred.	η_{ex} Error (%)	$\dot{Q}_{dest}$ Error (%)
1000	1.0	25	0.01621	4.23	7.1	12.40	5.99	2.50	12.24	-15.69	-1.28
1000	1.0	50	0.03243	3.47	15.7	15.41	16.60	2.74	15.53	5.72	0.81
1000	1.0	75	0.04864	2.35	27.3	23.20	27.03	3.15	23.37	-1.00	0.75
1000	1.0	100	0.06485	1.79	31.9	31.59	32.77	3.46	31.73	2.74	0.46
2000	2.0	25	0.02190	5.20	5.3	17.44	4.90	2.85	17.35	-7.62	-0.53
2000	2.0	50	0.04038	3.57	22.4	26.48	22.31	3.26	26.16	-0.39	-1.19
2000	2.0	75	0.06056	2.41	32.3	41.41	31.51	3.71	40.95	-2.46	-1.11
2000	2.0	100	0.08075	1.84	35.1	56.94	35.03	4.05	57.28	-0.19	0.61
3000	3.0	25	0.02416	4.67	11.6	30.07	14.11	3.45	31.42	21.62	4.48
3000	3.0	50	0.04833	2.40	32.3	61.58	32.29	4.12	61.70	-0.04	0.20
3000	3.0	75	0.07249	1.63	34.8	95.57	34.05	4.54	93.50	-2.15	-2.17
3000	3.0	100	0.09665	1.24	32.7	129.90	32.14	4.86	129.65	-1.71	-0.20
4000	4.0	25	0.02814	4.58	17.5	52.35	15.89	3.93	50.95	-9.23	-2.67
4000	4.0	50	0.05628	2.34	29.9	102.26	30.37	4.63	102.87	1.58	0.60
4000	4.0	75	0.08441	1.61	26.9	154.64	27.15	5.06	157.05	0.92	1.56
4000	4.0	100	0.11255	0.92	20.6	256.35	20.94	5.54	255.81	1.67	-0.21

Table A4. Comparison of present work with previous experimental similar studies

Exergy	This Study (Full Load)				Bahar Sayin Kul 1 and Ali Kahraman		Chandrabhushan Tiwari et al.	N. M. AL-NAJEM and J. M. DIAB
	1000 rpm	2000 rpm	3000 rpm	4000 rpm	1400 rpm	2800 rpm	1500 rpm	-
Work Exergy (%)	31.93	35.12	32.72	20.59	29.38	29.47	31.06	34.33
Heat related Exergy (%)	3.18	2.19	1.78	1.40	5.58	5.32	4.43	-
Exergy Exhaust (%)	20.98	21.72	22.94	24.10	13.45	13.79	18.35	11.41
Exergy Destruction (%)	43.91	40.97	42.56	53.91	51.60	51.43	46.14	49.36
Exergetic Efficiency (%)	31.93	35.12	32.72	20.59	29.20	26.0	31.06	-